RESEARCH ARTICLE

Small-worldness of brain networks after brachial plexus injury: a resting-state functional magnetic resonance imaging study

Wei-Wei Wang[1], Ye-Chen Lu[2], Wei-Jun Tang[1], Jun-Hai Zhang[1], Hua-Ping Sun[1], Xiao-Yuan Feng[1], Han-Qiu Liu[1,*]
1 Department of Radiology, Huashan Hospital, Fudan University, Shanghai, China
2 Department of Hand Surgery, Huashan Hospital, Fudan University, Shanghai, China

Graphical Abstract

The varied small-worldness in brachial plexus injury (BPI) patients and healthy controls

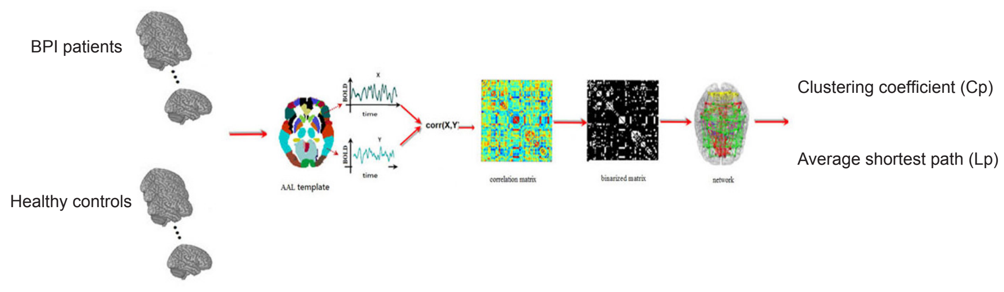

***Correspondence to:**
Han-Qiu Liu, Ph.D.,
drliuhanqiu@163.com.

orcid:
0000-0001-8294-6956
(Han-Qiu Liu)

doi: *10.4103/1673-5374.233450*

Accepted: *2018-05-02*

Abstract

Research on brain function after brachial plexus injury focuses on local cortical functional reorganization, and few studies have focused on brain networks after brachial plexus injury. Changes in brain networks may help understanding of brain plasticity at the global level. We hypothesized that topology of the global cerebral resting-state functional network changes after unilateral brachial plexus injury. Thus, in this cross-sectional study, we recruited eight male patients with unilateral brachial plexus injury (right handedness, mean age of 27.9 ± 5.4 years old) and eight male healthy controls (right handedness, mean age of 28.6 ± 3.2). After acquiring and preprocessing resting-state magnetic resonance imaging data, the cerebrum was divided into 90 regions and Pearson's correlation coefficient calculated between regions. These correlation matrices were then converted into a binary matrix with affixed sparsity values of 0.1–0.46. Under sparsity conditions, both groups satisfied this small-world property. The clustering coefficient was markedly lower, while average shortest path remarkably higher in patients compared with healthy controls. These findings confirm that cerebral functional networks in patients still show small-world characteristics, which are highly effective in information transmission in the brain, as well as normal controls. Alternatively, varied small-worldness suggests that capacity of information transmission and integration in different brain regions in brachial plexus injury patients is damaged.

Key Words: *nerve regeneration; brachial plexus injury; functional magnetic resonance imaging; small-world network; small-world property; topology properties; functional reorganization; clustering coefficient; shortest path; peripheral nerve injury; neural regeneration*

Introduction

Brachial plexus injury (BPI) is a severe peripheral nerve injury that results in complete or partial functional paralysis, and which may accompany mental disorders (Zhang and Gu, 2011; Yang et al., 2015a, b). Although peripheral surgery can be performed, understanding cerebral plasticity may be an option for promoting development of new treatments and interventions (Lundborg, 2000; Fraiman et al., 2016). Previous studies have mainly focused on cortical functional remodeling and connectivity. Moreover, animal studies have confirmed interhemispheric functional reorganization after complete nerve transection and surgical repair (Condés-Lara et al., 2000). Human brain imaging studies have corroborated these findings from animal models, showing loss of interhemispheric cortical inhibition after BPI (Hsieh et al., 2002). With the development of functional connectivity magnetic resonance imaging (MRI), a growing number of researchers are recognizing that brain regions are not independent, and instead perform their functions *via* complex network systems (Pawela et al., 2010; Brier et al., 2012; Liu et al., 2013).

Alterations in functional connectivity of distributed brain system in patients with BPI have recently attracted more investigative attention, yet it remains unclear whether peripheral nerve injury causes changes within the whole functional brain network. The small-world network is an important model for describing complex brain networks by specific features, namely high clustering coefficients (Cp) and average shortest paths (Lp) (Bullmore and Sporns, 2009). In addition, brain network connections can be measured by quantitative parameters (Bassett and Bullmore, 2006). Currently, a number of studies have demonstrated the complexity of brain networks with small-world network topology properties in healthy and diseased states (Liu et al., 2012; Ahmadlou et al., 2013; Bolaños et al., 2013).

Here, we hypothesized that: (1) both patients with BPI and normal controls would be characterized by small-world attributes; and (2) we also expected to demonstrate altered small-world parameters among patients and normal controls. This study compares changes in cerebral functional networks between patients with unilateral BPI and normal controls using resting-state functional connectivity MRI to investigate variable small-world parameters.

Participants and Methods

Participants

Our research was approved by the Medical Ethics Committee of Fudan University of China (approval No. 2016-060). Before the experiment, informed consent was provided by the subjects, who were all admitted to the Department of Hand Surgery, Huashan Hospital, Fudan University, China. The sample size was in accordance with a previous study (Guo et al., 2014). Eight male patients (right-handed, mean age: 27.9 ± 5.4 years) who suffered from unilateral BPI participated in this cross-sectional study. All were from Huashan Hospital, Fudan University. MRI scanning was performed one to six months after injury. Eight healthy right-handed and age-matched (mean age: 28.6 ± 3.2 years) subjects served as healthy controls.

Inclusion criteria

Patients who met all of the following criteria were considered for study inclusion: total brachial plexus root avulsion diagnosed in accordance with a previous study (Zhang and Gu, 2011); and physical examination and electromyography of the affected upper extremity demonstrated lateral total brachial plexus avulsion injury.

Exclusion criteria

Patients who met one or more of the following conditions were excluded from the study: contraindications of MRI; organic pathological brain changes; history of central nervous system disease, such as mental illness or stroke; or history of chronic diseases such as diabetes.

Preoperative resting-state functional magnetic resonance imaging (fMRI) was performed. The whole brachial plexus was exposed during surgery. Accurate diagnosis of total brachial plexus root avulsion was made during the operation (Yang et al., 2015a, b).

Demographic characteristics of the patients are shown in **Table 1**.

Data acquisition and preprocessing

Images were collected on a MR scanner (3-Tesla, Discovery MR750; GE Medical Systems, Milwaukee, WI, USA), with the participants in a supine position and foam pillows used to avoid head motion. The subjects were in a blank state (not yet affected by experiences or impressions), lying on the examination table with their eyes closed but not asleep. Resting-state fMRI images were obtained using a gradient echo-planar imaging sequence. The parameters were as follows: repetition time: 2000 ms, angle acquisition matrix: 64 × 64, flip angle: 75°, echo time: 35 ms, slice thickness: 5 mm, interslice space: 0 mm, and field of view: 240 mm × 240 mm. Resting-state images were analyzed with a Graph-theoretical Network Analysis Toolkit (GRETNA, www.nitrc.org), based on Statistical Parametric Mapping (SPM)-8 (Version 8, implemented in Matlab 7.1.1 [R2010b]; http://www.fil.ion.ucl.ac.uk/spm/, provided by Department of Psychiatry, University of Jena, Jena, Germany). The first 10 images were removed to maintain magnetization equilibrium. First, slice timing in SPM8 was performed to eliminate differences in acquisition time for each aspect of the image. Second, conventional realigned time-series images were acquired by removing fMRI movement artifacts based on least squares and rigid body transformation. Third, normalization of resampled images was performed in a selected standard space (provided by the Montreal Neurological Institute) with voxel sizes of 3 × 3 × 3 mm^3. The linear trend was removed after normalizing by detrending. Finally, high frequency noise was eliminated using a band-pass filter (0.01–0.08 Hz).

Anatomical parcellation and graph construction

Before constructing functional networks, the whole cerebrum was divided into 90 symmetrical areas using the automated anatomical labeling atlas (Tzourio-Mazoyer et al., 2002). Signals were obtained of all voxels among every area of mean time series. Linear regression was then used to remove covariants, specifically, head movement parameters, white matter, and cerebrospinal fluid signal. A partial correlation matrix (R) between every pair of brain areas was acquired by calculating Pearson's correlation coefficient. Fisher's transformation was then applied. By choosing the threshold sparsity, the paired correlation matrix was transformed into binary matrices. Every correlation matrix was repeatedly obtained in a chosen width of sparsity: 10–46% with intervals of 0.01. Binary graphs were obtained from the sparsity threshold, in which brain regions were expressed in nodes and functional relationships between brain regions expressed in edges (Yao et al., 2015; Bassett and Bullmore, 2016; Muldoon et al., 2016).

Small-world analysis

Four parameters were used to depict whole topological properties of the global cerebral resting-state functional network: Cp, Lp, normalized Cp (γ), and normalized Lp (λ). Cp is defined as the average clustering coefficient of all nodes in the network. The clustering coefficient, Ci, of node I was calculated as Ci = 2Ei / Ki × (Ki – 1), where Ei represents the number of edges existing between node I's neighbor nodes, and Ki the degree of node i. Lp is the average number of edges along the shortest path for all possible pair of nodes. Full Unicom's network is a fully connected mesh network with a direct link in each node. However, within the non-full Unicom's network, there is no connection between two nodes, and the Lp of such nodes that do not connect to each other is infinite. Accordingly, Newman (2003) proposed to

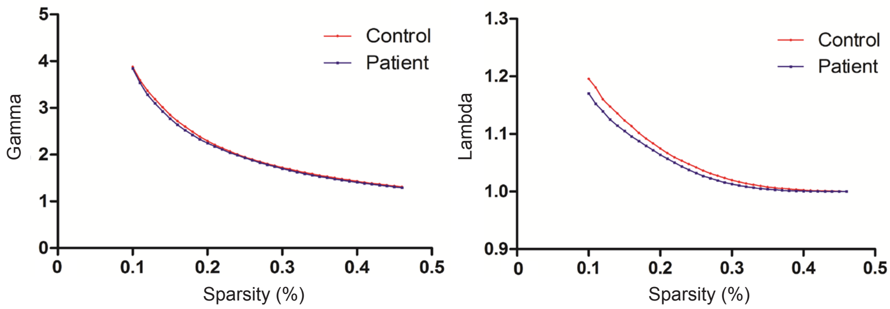

Figure 1 Whole topological properties of the global cerebral resting-state functional network: λ and γ in patients with brachial plexus injury and normal controls.
Under sparsity conditions of 0.1–0.46, both groups showed γ = Cpreal / Cprand >1 and λ = Lpreal / Lprand ≈ 1.

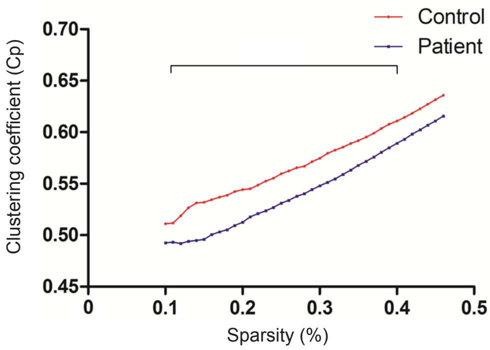

Figure 2 Average clustering coefficient of all nodes in the brain network: Cp in patients with brachial plexus injury and normal controls.
Clustering coefficient (Cp) of patients with unilateral brachial plexus injury was significantly lower compared with healthy controls: 0.11 ≤ sparsity ≤ 0.4 ($P < 0.05$).

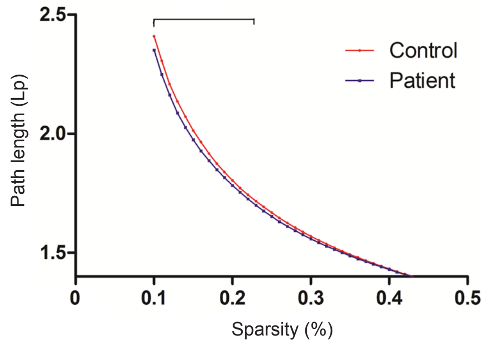

Figure 3 Average number of edges along shortest paths for all possible pair of nodes in the brain network: Lp in patients with brachial plexus injury and normal controls.
Significant differences were detected for average shortest path (Lp) at 0.1 ≤ sparsity ≤ 0.23, with Lp of brachial plexus injury patients being higher than controls.

Table 1 Demographic characteristics of the patients

Case	Age (year)	Handedness	Lesions	Time course for fMRI (month)
1	25	Right	Total avulsion, right	1
2	37	Right	Total avulsion, right	1
3	22	Right	Total avulsion, right	4
4	23	Right	Total avulsion, right	3
5	30	Right	Total avulsion, right	1
6	34	Right	Total avulsion, right	1
7	25	Right	Total avulsion, right	2
8	27	Right	Total avulsion, right	1

fMRI: Functional magnetic resonance imaging.

use the harmonic mean path between these network nodes to measure Lp and avoid this problem. Cp represents the level of local information transfer efficiency in a network, while Lp measures global efficiency of the brain network (Latora and Marchiori, 2001). The small-world network is an important model for describing complex brain networks with the criteria: γ > 1 and λ ≈ 1 (Watts and Strogatz, 1998) or σ = γ / λN1 (Humphries et al., 2006). To test small-world characteristics, normalized γ = Cpreal / Cpr and normalized λ = Lpreal / Lprand were calculated (Bullmore and Sporns, 2009). Cpreal and Lpreal represent Cp and Lp of real networks, respectively. The matched random network has the same number of nodes, edges, and degree distribution as the real network. Cprand and Lprand are the corresponding indices of random networks by repeating 100 times (Maslov and Sneppen, 2002; Milo et al., 2002). Cprand and s of Lprand are used to calculate Lp and Cp, random network node and edge number, and distribution network with true equality (Bassett and Bullmore, 2006; Shim et al., 2014; Muldoon et al., 2016).

Statistical analysis

GraphPad prism v5.0 (GraphPad Software, Inc., La Jolla, CA, USA) was used to calculate group differences in topological properties of the global cerebral functional network, with Cp and Lp assessed using two sample *t*-tests ($P < 0.05$). This test procedure was practiced at each selected threshold value (0.1–0.46) to obtain statistical differences between the two groups.

Results

Small-worldness of brain networks in patients with BPI and normal controls

Both γ and λ were calculated in patients with BPI and controls. Sparsity was set at 0.1–0.46, with intervals of 0.01. Both groups showed γ = Cpreal / Cprand > 1 and λ = Lpreal / Lprand ≈ 1, showing that both groups meet the small-world criteria (**Figure 1**).

Altered small-world properties of both groups

Next, we calculated Cp and Lp, and compared them between patients with BPI and controls using two sample *t*-tests. In both groups, Cp increased while Lp decreased along with increasing threshold. In patients with unilateral BPI, Cp was significantly lower compared with healthy controls: 0.11 ≤ sparsity ≤ 0.4 ($P < 0.05$; **Figure 2**). Meanwhile, significant differences were detected with average Lp: 0.1 ≤ sparsity ≤ 0.23, with Lp being higher in patients than controls (**Figure 3**).

Discussion

Graph-based network analysis is becoming an important fMRI method (He et al., 2008; Wang et al., 2010; Zhou and Lui, 2013; Yao et al., 2015). Graph theory is based on graphically representing the complexity of the brain by nodes and edges (Oliveira, 2012; Bassett and Bullmore, 2016). Small-world network models are important for characterizing complex brain networks. Previous studies have shown that healthy people, and even patients with Alzheimer's disease (Liu et al., 2012; Dennis and Thompson, 2014; Jia et al., 2016) or attention-deficit hyperactivity disorder (Wang et al., 2009; Jacot et al., 2016), have complex and highly efficient neural architectures, with maximum capacity to process information with large Cp and short Lp. Here, both groups showed efficient small-world structure with sparsity setting at 0.1–0.46. Thus, although peripheral nerve injury induces removal of sensory inputs and blockage of motor output activity, there is no obvious influence on effective information transfer of the whole brain network. This is the first time that topological properties of the whole cerebral network have been studied in patients with BPI.

Graph theoretical analysis reveals abnormalities in multiple network attributes. It has been shown that small-world network properties, such as Cp, decrease significantly in patients with AD, implying disrupted local network connectivity (Supekar et al., 2008). Besides, Lp decreased significantly in patients with medial temporal lobe epilepsy (Liao et al., 2010). Similarly, internal characteristics of brain small-world networks have changed. We found that patients with BPI have smaller Cp and larger Lp within a wide sparsity range. Cp measures local information transfer capability of a network. A smaller clustering coefficient, indicating relatively sparse local connection of brain networks, reflects inferior processing ability of local information in patients with BPI. Lp represents global efficiency of brain networks. Longer Lp may indicate that information interactions between brain regions are slower and less efficient in patients, because information is exchanged *via* more steps. This was the first time that changes in a global cerebral small-world network have been investigated in patients with peripheral nerve injury. Accordingly, resting-state functional brain connectivity features have been identified, which will facilitate our understanding of complex brain networks.

Loss of afferent input causes interruption of interhemispheric sensorimotor cortical connectivity (Qiu et al., 2014) and reduced functional connectivity between bilateral primary motor cortex after brachial plexus root avulsion (Liu et al., 2013). Altogether, these results show reduction of long distance brain function connectivity in BPI sufferers. In addition, resting-state MRI showed an altered local functional network in patients with BPI compared with healthy subjects in the bilateral fronto-parietal network, sensorimotor network, and executive-control network (Feng et al., 2016). Consequently, smaller Cp and longer Lp suggest significantly disrupted local and global network connectivity in sufferers with brachial plexus nerve avulsion compared with control subjects.

This study has limitations. Only eight subjects were recruited and a study with a larger sample size is needed. Additionally, it is known that functional reorganization occurs after BPI and contralateral C_7 nerve root transfer. However, it is still unknown how the topology of the global cerebral resting-state functional network changes after nerve repair, which may be associated with brain functional reorganization after BPI. It is noteworthy that right BPI induced a greater extent of brain functional reorganization than left injury (Feng et al., 2015). To avoid this, the patients in our study all experienced right BPI and differences in the brain network of patients with unilateral BPI depends on further investigation.

This is the first study to examine the topology of the global cerebrum in patients with unilateral BPI. Our results suggest that effective small-worldness of brain functional networks is not changed in patients, while internal characteristics of brain small-world networks are varied. This study may help understanding of functional reorganization after BPI from the perspective of networks.

Acknowledgments: *The authors would like to thank Yun Li for writing assistance. Yun Li is a foreign student from the Department of Radiology, Huadong Hospital, Fudan University, China.*
Author contributions: *XYF and HQL conceived and designed the experiments. WWW and YCL performed the experiments. WWW and WJT analyzed the data. JHZ and HPS provided reagents/materials/analysis tools. WWW wrote the paper. All authors approved the final version of the paper.*
Conflicts of interest: *The authors declare that the research was conducted in the absence of any commercial or financial relationships that could be construed as a potential conflict of interest.*
Financial support: *None.*
Institutional review board statement: *The study followed international and national regulations in accordance with the Declaration of Helsinki and relevant ethical principles. The study was approved by the Medical Ethics Committee of Fudan University of China (approval No. 2016-060).*
Declaration of participant consent: *The authors certify that they have obtained all appropriate participant consent forms. In the form, the participants have given their consent for their images and other clinical information to be reported in the journal. The patients have understood that their names and initials would not be published and due efforts would be made to conceal their identity, but anonymity cannot be guaranteed.*
Reporting statement: *This study follows the Recommendations for the Conduct, Reporting, Editing and Publication of Scholarly Work in Medical Journals developed by the International Committee of Medical Journal Editors.*
Biostatistics statement: *The statistical methods of this study were reviewed by the biostatistician of Department of Radiology, Huashan Hospital, Fudan University, Shanghai, China.*
Copyright license agreement: *The Copyright License Agreement has been signed by all authors before publication.*
Data sharing statement: *Datasets analyzed during the current study are available from the corresponding author on reasonable request.*
Plagiarism check: *Checked twice by iThenticate.*
Peer review: *Externally peer reviewed.*

References

Ahmadlou M, Ahmadi K, Rezazade M, Azad-Marzabadi E (2013) Global organization of functional brain connectivity in methamphetamine abusers. Clin Neurophysiol 124:1122-1131.

Bassett DS, Bullmore E (2006) Small-world brain networks. Neuroscientist 12:512-523.

Bassett DS, Bullmore ET (2016) Small-world brain networks revisited. Neuroscientist 23:499-516.

Bolaños M, Bernat EM, He B, Aviyente S (2013) A weighted small world network measure for assessing functional connectivity. J Neurosci Methods 212:133-142.

Brier MR, Thomas JB, Snyder AZ, Benzinger TL, Zhang D, Raichle ME, Holtzman DM, Morris JC, Ances BM (2012) Loss of intranetwork and internetwork resting state functional connections with Alzheimer's disease progression. J Neurosci 32:8890-8899.

Bullmore E, Sporns O (2009) Complex brain networks: graph theoretical analysis of structural and functional systems. Nat Rev Neurosci 10:186-198.

Condés-Lara M, Barrios FA, Romo JR, Rojas R, Salgado P, Sánchez-Cortazar J (2000) Brain somatic representation of phantom and intact limb: a fMRI study case report. Eur J Pain 4:239-245.

Dennis EL, Thompson PM (2014) Functional brain connectivity using fMRI in aging and Alzheimer's disease. Neuropsychol Rev 24:49-62.

Feng JT, Liu HQ, Xu JG, Gu YD, Shen YD (2015) Differences in brain adaptive functional reorganization in right and left total brachial plexus injury patients. World Neurosurg 84:702-708.

Feng JT, Liu HQ, Hua XY, Gu YD, Xu JG, Xu WD (2016) Brain functional network abnormality extends beyond the sensorimotor network in brachial plexus injury patients. Brain Imaging Behav 10:1198-1205.

Fraiman D, Miranda MF, Erthal F, Buur PF, Elschot M, Souza L, Rombouts SA, Schimmelpenninck CA, Norris DG, Malessy MJ, Galves A, Vargas CD (2016) Reduced functional connectivity within the primary motor cortex of patients with brachial plexus injury. Neuroimage Clin 12:277-284.

Guo Q, Thabane L, Hall G, McKinnon M, Goeree R, Pullenayegum E (2014) A systematic review of the reporting of sample size calculations and corresponding data components in observational functional magnetic resonance imaging studies. Neuroimage 86:172-181.

He Y, Chen Z, Evans A (2008) Structural insights into aberrant topological patterns of large-scale cortical networks in Alzheimer's disease. J Neurosci 28:4756-4766.

Hsieh JC, Cheng H, Hsieh HM, Liao KK, Wu YT, Yeh TC, Ho LT (2002) Loss of interhemispheric inhibition on the ipsilateral primary sensorimotor cortex in patients with brachial plexus injury: fMRI study. Ann Neurol 51:381-385.

Humphries MD, Gurney K, Prescott TJ (2006) The brainstem reticular formation is a small-world, not scale-free, network. Proc Biol Sci 273:503-511.

Jacot W, Firmin N, Roca L, Topart D, Gallet S, Durigova A, Mirr S, Abach L, Pouderoux S, D'Hondt V, Bleuse JP, Lamy PJ, Romieu G (2016) Impact of a tailored oral vitamin D supplementation regimen on serum 25-hydroxyvitamin D levels in early breast cancer patients: a randomized phase III study. Ann Oncol 27:1235-1241.

Jia Y, Nie K, Li J, Liang X, Zhang X (2016) Identification of therapeutic targets for Alzheimer's disease via differentially expressed gene and weighted gene co-expression network analyses. Mol Med Rep 14:4844-4848.

Latora V, Marchiori M (2001) Efficient behavior of small-world networks. Phys Rev Lett 87:198701.

Liao W, Zhang Z, Pan Z, Mantini D, Ding J, Duan X, Luo C, Lu G, Chen H (2010) Altered functional connectivity and small-world in mesial temporal lobe epilepsy. PLoS One 5:e8525.

Liu B, Li T, Tang WJ, Zhang JH, Sun HP, Xu WD, Liu HQ, Feng XY (2013) Changes of inter-hemispheric functional connectivity between motor cortices after brachial plexuses injury: a resting-state fMRI study. Neuroscience 243:33-39.

Liu Z, Zhang Y, Yan H, Bai L, Dai R, Wei W, Zhong C, Xue T, Wang H, Feng Y, You Y, Zhang X, Tian J (2012) Altered topological patterns of brain networks in mild cognitive impairment and Alzheimer's disease: a resting-state fMRI study. Psychiatry Res 202:118-125.

Lundborg G (2000) Brain plasticity and hand surgery: an overview. J Hand Surg Br 25:242-252.

Maslov S, Sneppen K (2002) Specificity and stability in topology of protein networks. Science 296:910-913.

Milo R, Shen-Orr S, Itzkovitz S, Kashtan N, Chklovskii D, Alon U (2002) Network motifs: simple building blocks of complex networks. Science 298:824-827.

Muldoon SF, Bridgeford EW, Bassett DS (2016) Small-world propensity and weighted brain networks. Sci Rep 6:22057.

Newman M (2003) The structure and function of complex networks. SIAM Rev Soc Ind Appl Math 45:167-256.

Oliveira J (2012) It's a Small World! Small 8:3-4.

Pawela CP, Biswal BB, Hudetz AG, Li R, Jones SR, Cho YR, Matloub HS, Hyde JS (2010) Interhemispheric neuroplasticity following limb deafferentation detected by resting-state functional connectivity magnetic resonance imaging (fcMRI) and functional magnetic resonance imaging (fMRI). Neuroimage 49:2467-2478.

Qiu TM, Chen L, Mao Y, Wu JS, Tang WJ, Hu SN, Zhou LF, Gu YD (2014) Sensorimotor cortical changes assessed with resting-state fMRI following total brachial plexus root avulsion. J Neurol Neurosurg Psychiatry 85:99-105.

Shim M, Kim DW, Lee SH, Im CH (2014) Disruptions in small-world cortical functional connectivity network during an auditory oddball paradigm task in patients with schizophrenia. Schizophr Res 156:197-203.

Supekar K, Menon V, Rubin D, Musen M, Greicius MD (2008) Network analysis of intrinsic functional brain connectivity in Alzheimer's disease. PLoS Comput Biol 4:e1000100.

Tzourio-Mazoyer N, Landeau B, Papathanassiou D, Crivello F, Etard O, Delcroix N, Mazoyer B, Joliot M (2002) Automated anatomical labeling of activations in SPM using a macroscopic anatomical parcellation of the MNI MRI single-subject brain. Neuroimage 15:273-289.

Wang L, Li Y, Metzak P, He Y, Woodward TS (2010) Age-related changes in topological patterns of large-scale brain functional networks during memory encoding and recognition. Neuroimage 50:862-872.

Wang L, Zhu C, He Y, Zang Y, Cao Q, Zhang H, Zhong Q, Wang Y (2009) Altered small-world brain functional networks in children with attention-deficit/hyperactivity disorder. Hum Brain Mapp 30:638-649.

Watts DJ, Strogatz SH (1998) Collective dynamics of 'small-world' networks. Nature 393:440-442.

Yang G, Chang KW, Chung KC (2015a) A systematic review of contralateral C7 transfer for the treatment of traumatic brachial plexus injury: Part 1. Overall Outcomes. Plast Reconstr Surg 136:794-809.

Yang G, Chang KW, Chung KC (2015b) A systematic review of outcomes of contralateral C_7 transfer for the treatment of traumatic brachial plexus injury: Part 2. Donor-Site Morbidity. Plast Reconstr Surg 136:480e-489e.

Yao Z, Hu B, Xie Y, Moore P, Zheng J (2015) A review of structural and functional brain networks: small world and atlas. Brain Inform 2:45-52.

Zhang CG, Gu YD (2011) Contralateral C_7 nerve transfer - Our experiences over past 25 years. J Brachial Plex Peripher Nerve Inj 6:10.

Zhou Y, Lui YW (2013) Small-world properties in mild cognitive impairment and early Alzheimer's disease: a cortical thickness MRI study. ISRN Geriatr 2013:542080.

(*Copyedited by James R, Wysong S, Yu J, Li CH, Qiu Y, Song LP, Zhao M*)